Magnetophonons in short-period superlattices

P. Gassot, J. Genoe,* D. K. Maude
High Magnetic Field Laboratory, Centre National de la Recherche Scientifique, Boîte Postale 166, 38042 Grenoble, France

J. C. Portal
High Magnetic Field Laboratory, Centre National de la Recherche Scientifique, Boîte Postale 166, 38042 Grenoble, France and Institut National des Sciences Appliquées, F-31077 Toulouse, France

K. S. H. Dalton, D. M. Symons,† and R. J. Nicholas
Clarendon Laboratory, Department of Physics, Oxford University, Parks Road, Oxford, OX1 3PU, United Kingdom

F. Aristone‡ and J. F. Palmier
France-Telecom, Paris-B, 196 Av. Henri Ravera, 92220 Bagneux, France

F. Laruelle
Laboratoire de Microstructures et de Microélectronique, Centre National de la Recherche Scientifique, 196 Avenue Henri Ravera, Boîte Postale 107, Paris-B, 92220 Bagneux, France

(Received 9 July 1996; revised manuscript received 12 August 1996)

We report the observation of magnetophonon resonances on the background of the longitudinal magnetoconductance in short-period GaAs/AlAs semiconductor superlattices. Both the GaAs and the AlAs longitudinal optical phonons are observed. We show how the enhancement of the magnetophonon effect with electric field is connected to the shift of the electron distribution towards the high-velocity and low-density-of-states region at the midpoint of the reduced Brillouin zone. The observed temperature dependence can be explained by considering the competition between the phonon population and the electron lifetime. The two superposed series of the GaAs and the AlAs optical phonons are shifted when hydrostatic pressure is applied and the relative strength of each series changes as the Γ miniband comes closer to the X states.
[S0163-1829(96)05844-4]

I. INTRODUCTION

Initially predicted by Gurevitch and Firsov[1] in 1961, the magnetophonon effect has been widely studied in bulk semiconductors. The oscillations in the magnetoresistance, caused by resonant scattering of electrons between Landau levels involving an interaction with optical phonons, has been used in order to investigate the electron properties as well as the lattice vibrations in many polar semiconductor materials.[2] At the end of the 1970s, new growth techniques such as molecular-beam epitaxy made it possible to obtain high-quality two-dimensional electron gases (2DEG's) and superlattices. Several experimental[3–5] and theoretical[6–10] papers on this effect in 2DEG's have been published, but relatively little attention has been devoted to short-period superlattices.[11]

In superlattices, the artificially induced periodicity breaks the conduction and the valence bands into minibands and minigaps. The electron dispersion relation is strongly nonparabolic along the growth axis.[12] The vertical transport, the so-called Bloch transport, is nonlinear due to the presence of an inflection point in the miniband. When a magnetic field is applied along the growth axis, clearly resolvable Landau levels are created in the plane of the layers when the cyclotron energy ($\hbar\omega_c$) is greater than the miniband width. The miniband is unchanged and the electronic system is fully quantized. In addition, the density of states presents singularities at the bottom and at the top of each Landau level.[11] Each time the energetic distance between two Landau levels corresponds to the energy of a longitudinal-optical (LO) phonon, the scattering mechanisms are enhanced and the magnetoresistance shows a local maximum.

In this paper we present the magnetophonon effect in short-period GaAs/AlAs superlattices resulting from electron interactions with both GaAs and AlAs LO phonons. Notably, we show how the electric field can have an influence on the strength of this effect by shifting the electron distribution towards the middle of the miniband where the electron drift velocity reaches a maximum and the density of states presents a minimum. We show that this phenomenon is more pronounced for narrow minibands. The observed temperature dependence can be explained by considering the competition between the thermal population of phonons and the thermal broadening of the Landau levels. Finally, we show how hydrostatic pressure allows us to resolve unequivocally the superposed AlAs and GaAs series of magnetophonon peaks.

II. SAMPLE DESCRIPTION

The three GaAs/AlAs superlattices investigated in this paper have been grown by molecular-beam epitaxy on a (001)-oriented Si-doped (2×10^{18} cm^{-3}) GaAs substrate. The structures (labeled A, B, and C) consist of 22/8, 22/5, and 19/7 monolayers of GaAs/AlAs, respectively. The superlat-

tices A and B are both lightly Si doped (10^{16} cm^{-3}), while C is 2×10^{16} cm^{-3} Si doped. The active region, embedded between n-type (2×10^{18} cm^{-3}) GaAs contact layers, is 1 μm thick. Layers of graded average composition, in the form of short-period superlattice quasialloys, have been grown between the n^+ contacts and the active region to avoid abrupt heterojunctions at the onset of the superlattice and to provide a continuous variation of the lowest conducting state between the contact and the superlattice. Electrically contacted mesas were fabricated using conventional processing techniques. The area of the mesa device is typically 2800 μm^2.

Vertical transport measurements are performed with a magnetic field applied parallel to the superlattice axis and supplied by a 15-T superconducting magnet, a 25-T resistive magnet, a 30-T hybrid magnet, and finally a 45-T pulsed magnet. For measurements under pressure an 11-kbar liquid clamp cell is used. Electrical access is available via electrical feedthroughs in an epoxy-sealed ''passage'' and the pressure is measured *in situ* by means of a calibrated InSb pressure gauge.

III. MODEL

A. Band structure and Landau level separation

We have calculated the band structure using the eight-band model described in Ref. 13. Figure 1 shows the band dispersion in the [001] and [100] directions.

This calculation allowed us to extract the miniband width (Δ), the in-plane effective mass ($m_\perp^*$), and the nonparabolicity of the in-plane direction (K_2^*). The energy dependence of the g factor[14] (K_0^*) has been determined from the $\mathbf{k}\cdot\mathbf{p}$ theory[15] by taking into account the confinement energy of the miniband and the energy of the longitudinal optical phonon. These parameters are shown in Table I. The values obtained for the in-plane mass are higher than the GaAs bulk effective mass at the same energy position due to the delocalization of the electronic wave function and thus its presence in the AlAs barrier.

In the absence of an applied magnetic field, the in-plane energy can be expressed as

$$E=E_0+\frac{\hbar^2k_\perp^2}{2m_\perp^*m_0}+K_2^*\frac{\hbar^4k_\perp^4}{4m_\perp^{*2}m_0^2}, \tag{1}$$

where $k_\perp$ is the momentum in the in-plane direction. We can express the effective g-factor as

$$g=g_0+K_0^*\frac{\hbar^2k_\perp^2}{2m_\perp^*m_0}. \tag{2}$$

The presence of a magnetic field will split the miniband into Landau levels (with index l)

$$E(l,\omega_c,\pm)=E_0+\hbar\omega_c(l+\tfrac{1}{2})+K_2^*\hbar^2\omega_c^2(l+\tfrac{1}{2})^2\pm g_0C_0\hbar\omega_c \pm K_0^*C_0\hbar^2\omega_c^2(l+\tfrac{1}{2}), \tag{3}$$

with $C_0=\mu_Bm_\perp^*/2\hbar e$, where μ_B is the Bohr magneton. The inset of Fig. 1 shows the calculated density of states under a magnetic field of 8.32 T. This field corresponds to the $N=3$ GaAs magnetophonon transition.

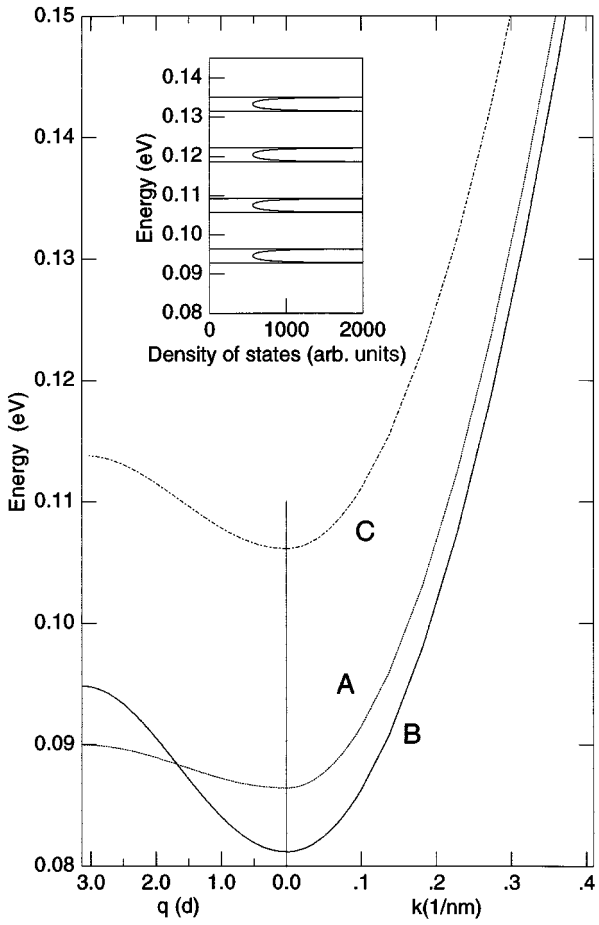

FIG. 1. Dispersion relations calculated using an eight-band model along the growth axis [001] (left-hand side) and in plane along the [100] axis (right-hand side). The inset shows the corresponding density of states for sample A at an applied magnetic field of 8.32 T corresponding to the $N=3$ magnetophonon resonance.

B. Superlattice phonons

In systems such as GaAs/AlAs where the optical phonon branches do not overlap, the phonon modes are confined in their own layer and are evanescent in the other layer.[18] This is in analogy with the electron in a quantum well embedded between two barriers. The optical modes are standing waves of X-Ga-As$\cdots$Ga-As-X and X-Al-As$\cdots$Al-As-X finite chains where the X's are infinitely heavy atoms in the GaAs and the AlAs layers, respectively. There are as many dispersionless modes as there are monolayers, i.e., 22 LO modes of GaAs phonons for samples A and B and 19 modes of GaAs phonons for sample C, all distributed in the energy range $E_{\rm LO}(q=2\pi/a)<\hbar\omega_{\rm LO}<E_{\rm LO}(q=0)$ and confined in the GaAs layer.[16,17] (q is the phonon wave vector and a is the

TABLE I. Calculated miniband parameters for the three samples investigated.

Sample	Δ (meV)	$m_\perp^*$	K_2^* (meV^{-1})	$K_0^*C_0$ (meV^{-1})
A	3.6	0.07469	−0.547284	0.04170
B	13.64	0.07388	−0.552442	0.04123
C	7.7	0.07618	−0.568145	0.04250

lattice parameter.) In the AlAs layer, eight, five, and seven confined modes are present for samples *A*, *B*, and *C*, respectively. Raman studies show that the main contribution to the resonance spectrum comes from the first LO mode at the top of the LO band, which corresponds to the bulk value. This has been attributed to the fact that the LO_1 phonon is the only mode for which the envelope has no node in the GaAs layer.[18] Moreover, this mode is symmetric with respect to the center of the quantum well, as is the electronic wave function. As a consequence, the LO_1 phonon confined in the GaAs layer, whose energy is 36.15 meV (291 cm^{-1}), dominates the interaction with electrons. For the longitudinal optical phonon of AlAs,[19] we also use the mode corresponding to the zone center of the bulk at 50 meV (402 cm^{-1}).

C. Superlattice polaron

In the quasiparticle approximation, the electron-phonon interaction induces a renormalization of the energy spectrum of the electrons.[20] This is called the polaron effect. The magnitude of this interaction is dependent on both the electron and the phonon concentration. However, the carrier concentrations used in samples *A*, *B*, and *C* are too small for the electron-electron interactions to play a significant role.

Here we use the superlattice polaron model, based upon the weak electron-phonon coupling, to introduce the electron-phonon interaction.[21] The polaron mass and energy (when only the interaction between one electron and one phonon is considered) are

$$E_l^R = E(l,\omega_c,\pm) + \Delta E, \tag{4}$$

$$\Delta E = \Delta E^0 + \Delta E', \tag{5}$$

$$\Delta E^0 = -\hbar\omega_0 F^0 \alpha, \tag{6}$$

$$\Delta E' = -F'\alpha \frac{\hbar^2 k_\perp^2}{2m_\perp^* m_0} = -F'\alpha\hbar\omega_c\left(l+\tfrac{1}{2}\right), \tag{7}$$

TABLE II. Calculated superlattice polaron corrections of the in-plane effective mass and the confinement energy for the three different samples.

Sample	F^0_{GaAs}	F'_{GaAs}	α_{GaAs}	F^0_{AlAs}	F'_{AlAs}	α_{AlAs}
A	1.5488	0.3719	0.08442	1.5534	0.3763	0.1041
B	1.4980	0.3287	0.08397	1.5125	0.3407	0.1036
C	1.5278	0.3530	0.08526	1.5367	0.3611	0.1052

where the polaron coupling constant[20] α can be expressed as (in SI units)

$$\alpha = \frac{e^2}{\hbar}\sqrt{\frac{m^*}{2\hbar\omega_{LO}}}\left(\frac{1}{\varepsilon_\infty^r}-\frac{1}{\varepsilon_S^r}\right)\frac{1}{4\pi\varepsilon_0}, \tag{8}$$

with ε_∞^r and ε_S^r the relative dielectric constants at high and low frequencies, respectively.

The values of F^0 and F' for our samples are given in Table II. Values between the bulk value (1 and $\frac{1}{6}$, respectively) and the 2DEG values ($\frac{\pi}{2}$ and $\frac{\pi}{8}$) are obtained. As expected, the values obtained are closer to their 2D equivalent because the major part of the wave function is present in the well.

The magnetophonon resonance is obtained when

$$\begin{aligned} E(l,\omega_c,\pm) - E(N,\omega_c,\pm) &= \hbar\omega_{LO} \\ &= \hbar\omega_c(l-N)[1-\alpha F' \pm K_0^* C_0 \hbar\omega_c \\ &\quad + K_2^*\hbar\omega_c(l+N+1)]. \end{aligned} \tag{9}$$

Due to the fact that the electron density is only 10^{16} cm^{-3} and that each Landau level is highly degenerate, for magnetic fields above 5 T, many electrons are in the lowest Landau level even at high temperature. For this case, the condition to have a magnetophonon resonance can be expressed as

$$\hbar\omega_c = \frac{(F'\alpha-1)+\sqrt{N^2(1-F'\alpha)^2+4\hbar\omega_{LO}N[K_2^*(N+1)\pm K_0^* C_0]}}{2N[K_2^*(N+1)\pm K_0^* C_0]}. \tag{10}$$

In Table III, we have calculated the magnetic fields corresponding to the different resonances.

D. Current-voltage characteristics

The vertical transport in short-period superlattices occurs via the so-called Bloch transport[22] in contrast with the hopping transport between Wannier-Stark quantized levels resulting from the localization in the electric field. Without any applied electric field, the average momentum of the distribution of electrons in the lowest conduction miniband at a given temperature *T* is zero. When an electric field is applied, following the theorem of acceleration, the average momentum increases and the distribution of electrons is globally shifted from the center towards the edge of the Brillouin zone. In the Ohmic regime, electrons probe the bottom of the miniband, which can be approximated by a parabola, and their velocity is, as a consequence, directly proportional to the electric field. As soon as the distribution of electrons approaches the inflection point of the miniband, the current-voltage characteristic becomes strongly nonlinear, passes through a maximum, and finally turns over into a negative differential conductance region. Using Chamber's equation,[23] it has been shown that the vertical current is proportional to

$$I_{vertical} \propto \frac{F^*}{1+F^{*2}}, \tag{11}$$

TABLE III. Calculated and experimental positions in the magnetic field (T) of the magnetophonon resonances. The + and − values are calculated using the ± in Eq. (10).

			Peak number (N)				
Sample	Mode	Value	1	2	3	4	5
A	GaAs	+	25.15	12.44	8.26	6.185	4.944
		−	25.24	12.46	8.27	6.191	4.947
		expt.	22.5	12.15	8.32	6.25	4.95
	AlAs	+	35.75	17.59	11.66	8.73	6.97
		−	35.95	17.63	11.68	8.74	6.98
		expt.	36.7	16.9			
B	GaAs	+	24.78	12.26	8.14	6.09	4.87
		expt.	22.7	12	8.08		-
	AlAs	+	35.22	17.33	11.49	8.60	6.87
		expt.		17			
C	GaAs	+	25.66	12.68	8.42	6.31	5.04
		expt.		12.5	8.72	6.58	-
	AlAs	+	36.5	17.94	11.9	8.90	7.11
		expt.		17.87			

where F^* can be expressed as

$$F^* = \frac{eFd\tau}{\hbar}, \tag{12}$$

with F, d, and τ the applied electric field, the superlattice periodicity, and the electronic lifetime, respectively. In the case where no Wannier Stark quantization is present, the current peaks at the voltage corresponding to $F^*=1$. The shift of this peak position with temperature gives the temperature dependence of the electronic lifetime, which can subsequently be used to analyze the temperature dependence of the magnetophonon effect.

IV. EXPERIMENTS

A. Miniband dependence

The current–magnetic-field (0–25 T) characteristics at different voltages, both in the Ohmic and in the nonlinear regime, have been measured at 285 K for the three different samples (A, B, and C). Inset (a) of Fig. 2 plots the longitudinal magnetoresistance of sample A. We note the presence of oscillations superposed on a quadratic background. From inset (b), it is clear that these oscillations are periodic in $1/B$ with a fundamental field of 25.44 T. The second derivatives of the longitudinal magnetoconductance $G=(I-I_0)/I_0$ (where I_0 is the intensity of the current without magnetic field) for the three samples under investigation is plotted in the main part of Fig. 2. The effect of the miniband width on the oscillations is evident. The superlattice with the smallest miniband (sample A) shows more pronounced peaks than the other two. These peaks occur around 4.95, 6.25, 8.32, 12.15, and 22.5 T, which correspond to the magnetophonon effect involving the LO phonons[11] of GaAs with electrons in the Γ miniband. Each time the energy between two Landau levels corresponds to the energy of a LO phonon, the scattering is enhanced and the magnetoresistance increases drastically.[11] Another peak, located around 17 T, is observed and we attribute this to the $N=2$ of the series involving the LO phonon of AlAs. Vertical transport experiments in pulsed magnetic field up to 45 T have been performed in order to verify this assumption. Figure 3 plots the measured magnetoconductance and its second derivative for a fixed value of the applied electric field in the nonlinear regime at room temperature. An additional peak, correspond-

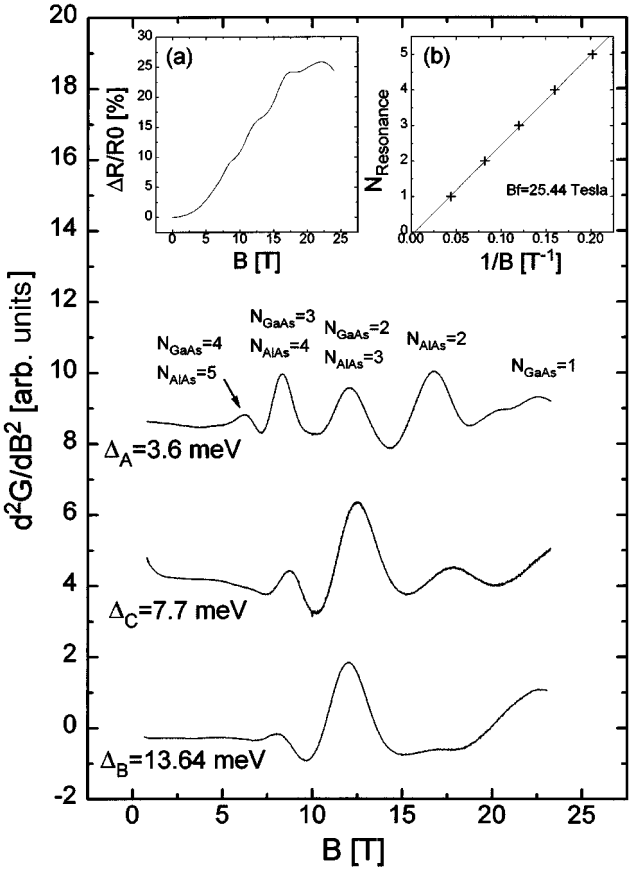

FIG. 2. Second derivative of the magnetoconductance versus the magnetic field for the three samples A, B and C at 285 K. The calculated miniband width is also indicated. Inset (a) plots the magnetoresistance versus the magnetic field at a voltage in the nonlinear regime. Inset (b) shows the resonance number versus $1/B$.

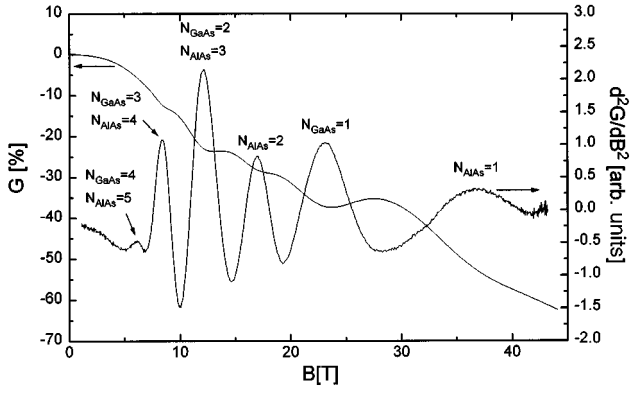

FIG. 3. Magnetoconductance and related second derivative versus the magnetic field up to 45 T for an applied voltage (0.7 V) in the nonlinear regime at room temperature.

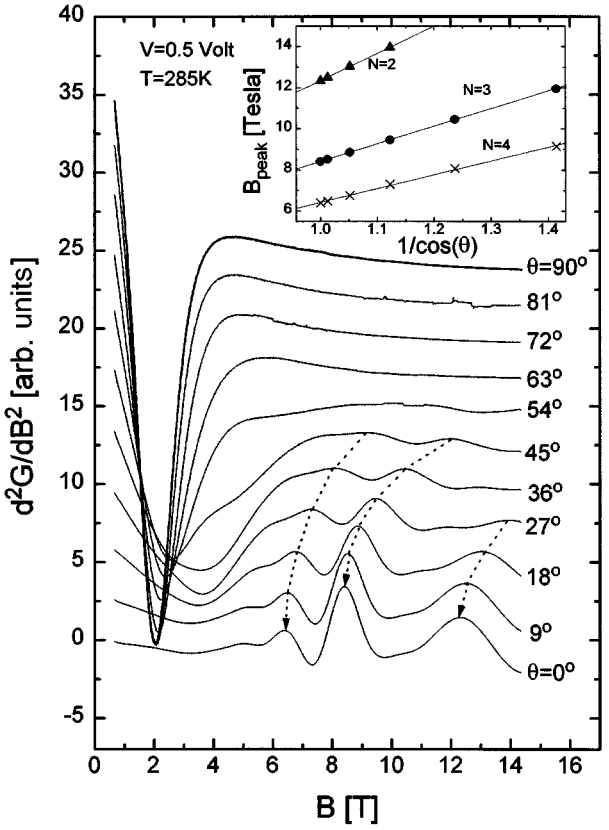

FIG. 4. Angular dependence of the magnetophonon resonances in sample *A* at $T=285$ K and 0.5 V. The inset plots the magnetic field of the different resonances of the GaAs LO phonon versus the inverse of the cosinus of the angle between the magnetic field and the axis of the superlattice.

ing to the $N=1$ of the AlAs series, is observed at 36.7 T. This clearly confirms the presence of two superposed series in our structures. The observation of the AlAs LO phonon originates from the overlap between the electron wave function that partially penetrates into the barriers and the AlAs phonon that is evanescent in the GaAs layer. A rotation of the magnetic field from *B* parallel to *B* perpendicular to the axis of the superlattice clearly shows that this effect is two dimensional. Figure 4 plots the second derivative of the magnetoconductance versus the magnetic field for different angles. There are no magnetophonon oscillations when the magnetic field is parallel to the layers ($\theta=90°$), as expected for a quasi-two dimensional system. Moreover, the minimum, observed at large angles and low magnetic fields in the second derivative of *G*, comes from the maximum of the magnetoconductance occurring in the crossed-fields configuration when the applied electric field is located in the nonlinear regime of the current-voltage characteristic. This effect, induced by a magnetic field applied parallel to the layers of a superlattice and due to the presence of a point of inflection in the dispersion along the growth axis, has been described theoretically using a semiclassical approach[24,25] and also observed experimentally.[26,27] Oscillations start to appear around 45°, but at higher magnetic field than for the magnetic field along the growth axis. The inset plots the position of different resonances versus $1/\cos(\theta)$. The linearity proves that this effect is purely two dimensional and that the Landau quantization occurs in the plane of the layers.

A comparison of the experimental results for sample *A* with the calculated values, including the nonparabolicity and the polaron correction described previously, shows good agreement for the high-order resonances and a nonnegligible discrepancy at the $N=1$ resonances. This peak shift has already been observed both in bulk semiconductors and in 2DEG's. This apparent anomaly stems from the fact that for both bulk semiconductors and 2DEG's the oscillatory part of the magnetoresistance can be represented by a Fourier series[28] whose main term is an exponentially damped cosinus. This exponential shifts[29] all the peak positions and preferentially the low-order ones. In addition, in our superlattices the presence of a smaller AlAs series of resonances superposed on the GaAs series further displaces the resonance peak positions. Experiments under hydrostatic pressure, which enhances the AlAs series, confirm this (see Sec. IV D). On the other hand, the miniband width dependence of this effect, presented in Fig. 2 for a fixed voltage, demonstrates that when a magnetic field is applied along the growth axis, isolated Landau levels are created in the plane of the layers when the cyclotron energy is greater than the miniband width. Moreover, scattering with optical modes is possible only within an energy range defined by

$$\hbar\omega_{\mathrm{LO}}-\Delta<N\hbar\omega_c<\hbar\omega_{\mathrm{LO}}+\Delta, \tag{13}$$

where Δ is the miniband width. The width of the magnetophonon resonances is, as a consequence, better resolved as the miniband width decreases. The oscillations of samples *B* and *C*, whose miniband widths are, respectively, 13.64 and 7.7 meV, are less pronounced compared to those of sample *A* ($\Delta=3.6$ meV). We also observe the influence of the in-plane effective mass on the position of the resonances. All the resonances of sample *C* are located at higher magnetic field compared to the other samples. In sample *C*, the first Γ miniband is 20 meV higher in energy than in the other superlattices and its in-plane effective mass is consequently larger (see Table I), which causes all the resonances to be shifted to higher magnetic fields.

B. Electric-field dependence

In this section we show the enhancement of the magnetophonon effect with the electric field. This effect is related to the high-velocity and low-density-of-states region in the middle of the miniband and to the shift of the electron distribution in the miniband as the voltage increases.

For all samples, we have observed that as the electric field across the structure increases, both the relative amplitude of the magnetophonon oscillations and the magnetoresistance background become more pronounced. Figure 5 shows the second derivative of the magnetoconductance versus the magnetic field for voltages in both the Ohmic and the nonlinear regime up to the current peak in the $I(V)$ characteristics. In contrast with recent experiments,[30] there is no shift of the resonances with the applied electric field, which indicates that no Wannier-Stark quantization occurs in our sample, even when the voltage drop per superlattice period reaches the same order of magnitude as the miniband width. The thermal broadening above 80 K is sufficient to prevent any

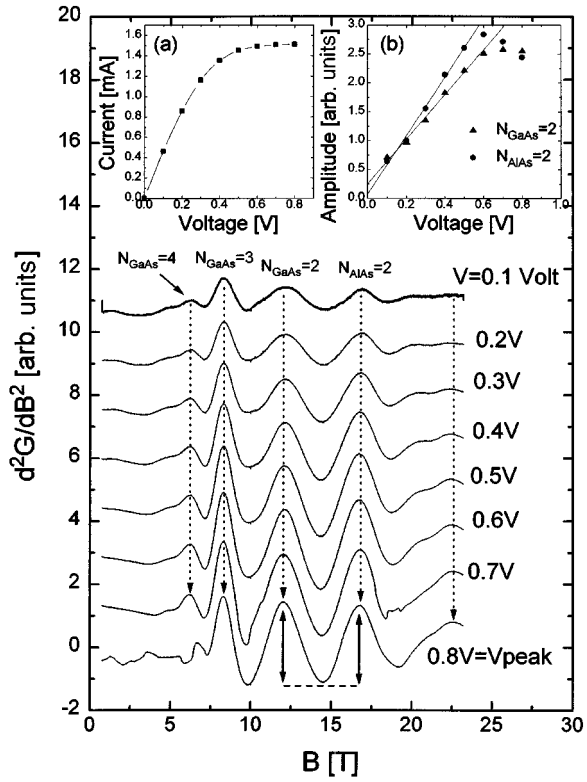

FIG. 5. Electric-field dependence of the magnetophonon effect for applied voltages in both the Ohmic and the nonlinear regimes at 250 K in sample *A*. Inset (a) plots the corresponding current-voltage characteristic and inset (b) plots the magnetophonon resonance amplitude as a function of the voltage for the $N=2$ peaks.

Wannier-Stark quantization and effectively preserves the miniband transport. The low amplitude of the oscillations below 80 K is also not consistent with transport dominated by hopping between Wannier-Stark levels. Moreover, Grahn *et al.*[31] have shown that the drift velocity of electrons in samples with small miniband width (0.5 and 1.5 meV) is well described by a Bloch transport picture for temperatures above 40 K. Thus we can be sure that we are not in a hopping regime.

Our oscillations, on the other hand, cannot be attributed to hot-electron magnetophonon resonances. These resonances have been widely studied,[10,32–34] and the mechanism requires that electrons, which are accelerated by the electric field, do not succeed in losing by scattering all the energy gained from the electric field. The temperature of the electron distribution increases until the difference from the lattice temperature is sufficiently large that energy relaxation via optical phonon emission is possible. At this threshold, an electron drops from a higher to a lower Landau level while emitting an optical phonon. The electron distribution is then cooled down to the lattice temperature. Two other hot-electron magnetophonon processes have also been reported: carrier trapping in a shallow impurity level and the emission of two TA phonons instead of an optical one. These effects have mainly been observed below 40 K, where almost no oscillations are present in our data.[2] Different models have shown that the heating of electrons in vertical transport in superlattices is miniband width dependent.[35,36] Suris and Shchamkhalova[35] showed that in the high-electric-field regime and without magnetic field, the electronic temperature T_e reaches a maximum

$$T_e = T\left[1+\left(\frac{\Delta}{2\hbar\omega_{L0}}\right)^2\right]. \tag{14}$$

From this expression, it is clear that the heating decreases with decreasing miniband width. This would be in disagreement with the experimentally observed increase in the amplitude of the oscillations with the decreasing miniband width and thus we conclude that the observed electric-field effect cannot be due to a hot magnetophonon effect.

Finally, our data cannot be explained by electric-field-induced elastic inter-Landau-level scattering (QUILLS).[37,38] First, the disappearance of the oscillations on the magnetoconductance below 80 K proves that the phenomenon really depends on the phonon population. Second, we observe that the position of the resonances measured between 1 and 8 kV/cm is the same as that measured for an applied electric field equal to 80 V/cm.[11] Thus there is no conversion from maxima to minima as observed by Eaves *et al.*[37] for QUILLS.

We believe the data can be explained by the simple picture of Bloch transport. In semiconductor superlattices, the electron distribution is shifted with the increasing applied electric field from the center of the Brillouin zone where the density of states presents a strong singularity to the inflection point of the dispersion relation where the density of states has a minimum and the electron velocity reaches a maximum. In this region, there are fewer free states available for scattering of the conducting electrons and the electron velocity reaches a maximum. When the possibility to absorb a LO phonon occurs, the scattering is enhanced and the magnetoresistance increases strongly, which leads to a peak. Moreover, we observe that the magnetoresistance also increases with the applied voltage. This is in contrast with the bulk magnetophonon effect, where both the initial and the final states lie in a high-density-of-states region. In the latter case, we would expect a better efficiency at low voltages where the electron distribution probes the singularity of the density of states. In our data, the amplitude of the effect increases linearly with the voltage through the Ohmic regime, saturates in the nonlinear regime up to a peak, and decreases afterward (see the inset of Fig. 5). This behavior is similar to the electric-field dependence of the average drift velocity of the electrons.

C. Temperature dependence

The longitudinal magnetoconductance of sample *A* has been measured for temperatures from 4.2 K to 285 K. Two different (low) electric fields were applied to confirm that the measurements are in the Ohmic regime of the current-voltage characteristics in the complete temperature range in order to be sure that the amplitude of the magnetophonon oscillations will remain linear in electric field for the whole temperature range. In this case, it is clear, since the amplitude of the magnetophonon effect depends on the position of the electron distribution relative to the minimum of the density of states, that this amplitude, for fixed applied voltage, will depend directly on the temperature dependence of the electron

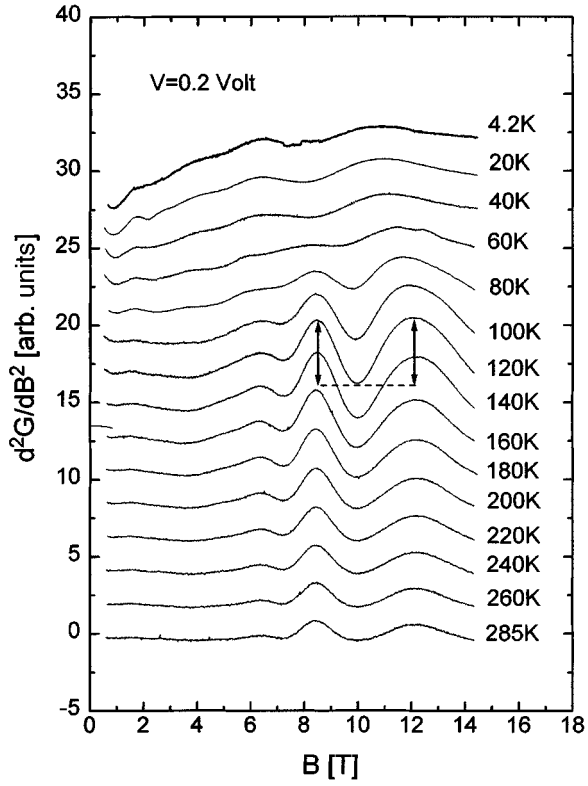

FIG. 6. Second derivative of the magnetoconductance versus the magnetic field for sample *A* at different temperatures between 4.2 and 285 K.

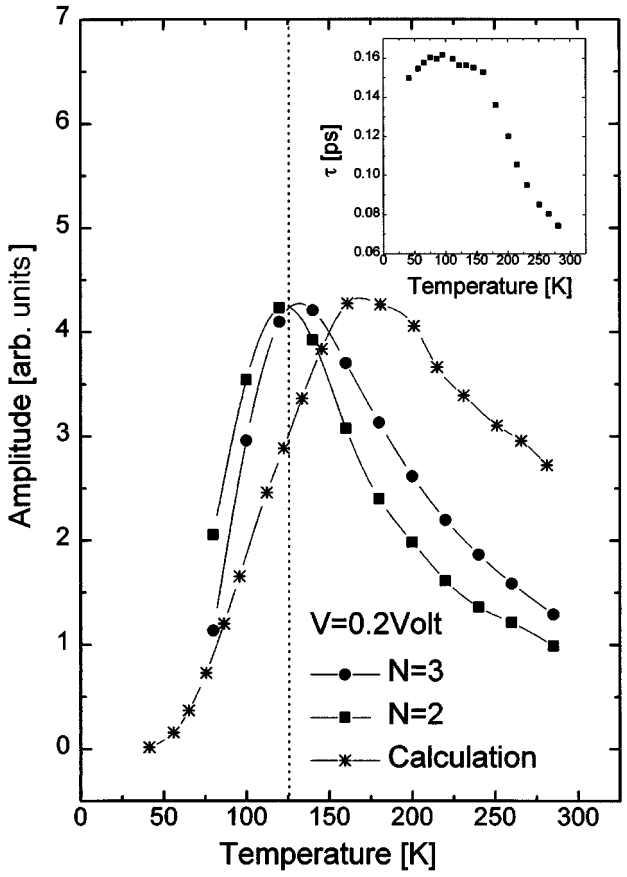

FIG. 7. Temperature dependence of the amplitude of both $N=2$ and 3 resonances of the GaAs series in sample *A*. The inset shows the electron lifetime derived from the current-voltage characteristics. This lifetime is used in the calculation of the expected temperature dependence.

lifetime. The second derivative of the measured magnetoconductance versus the magnetic field (see Fig. 6) is used to extract the magnetophonon oscillations. Figure 7 plots the amplitude as a function of temperature for the $N=2$ and 3 resonances of the GaAs series. At low temperature, the amplitude of the magnetophonon oscillations is small and mixed with Shubnikov–de Haas–like oscillations that result from a modulation of the electron injection from the n^+ GaAs contact. Above 80 K, the magnetophonon effect dominates. The amplitude of the oscillations increases strongly up to a maximum around 125 K, after which it decreases slowly as the temperature increases further. The temperature dependence of the magnetophonon effect reflects the competition between the thermal population of phonons and the transport lifetime of the electron. The amplitude of these oscillations decreases at high temperature because the linewidth of the Landau levels increases progressively due to thermal broadening and due to the fact that the shift of the electron distribution towards the center of the brillouin zone is reduced for shorter electron lifetimes. Moreover, the distribution function around the quasi Fermi level favors intraminiband scattering rather than inter-Landau-level scattering when the temperature increases. These three reasons lead to a diminished interaction with optical phonons even though the phonon population increases at high temperatures. In contrast, at low temperature, the Landau levels are well resolved, but there is a lack of optical modes whose typical temperature is around 417 K for GaAs and 580 K for AlAs. This dependence contrasts with previous results obtained by Noguchi *et al.*,[11] who observed a monotonic increase in amplitude of the magnetophonon resonances with increasing temperature and no oscillatory structure below 155 K. We do not understand the reason for this strange temperature dependence reported by Noguchi *et al.* However, as we will see below, our results are in good agreement with theory.

Gurevitch and Firsov[1] derived an approximate relation for the temperature dependence of the amplitude of the oscillatory term in bulk materials. Since the essential physics is the same, it should be applicable for superlattices. This relation can be expressed as[39]

$$\frac{\Delta\rho^{\mathrm{osc}}}{\rho}\propto\left(\frac{\hbar\omega_{\mathrm{LO}}}{kT}\right)^{3/2}\omega_c\tau(T)\exp\left(-\frac{\hbar\omega_{LO}}{kT}\right)\ln\left(\frac{kT}{\hbar}\tau(T)\right), \tag{15}$$

where $\tau(T)$ is the electronic lifetime, which depends on the temperature. This dependence has been extracted, as explained above, from the variation of the voltage position of the vertical current peak with the temperature (see inset of Fig. 7). The calculated temperature dependence of the magnetophonon effect is plotted in Fig. 7 to enable a comparison with our experimental results. Qualitative agreement is found even though the calculated maximum is shifted to higher temperature and is not as sharp as obtained experimentally. Equation (15) does not take into account the width of the miniband, which is possibly responsible for this discrepancy.

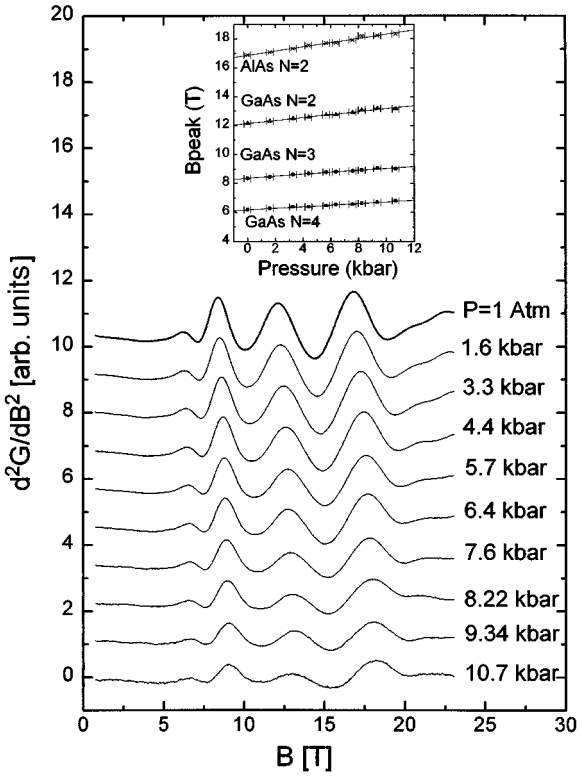

FIG. 8. Second derivative of the magnetoconductance of sample *A* under hydrostatic pressure up to 10.65 kbar, for a fixed value of the applied voltage in the nonlinear regime at 285 K.

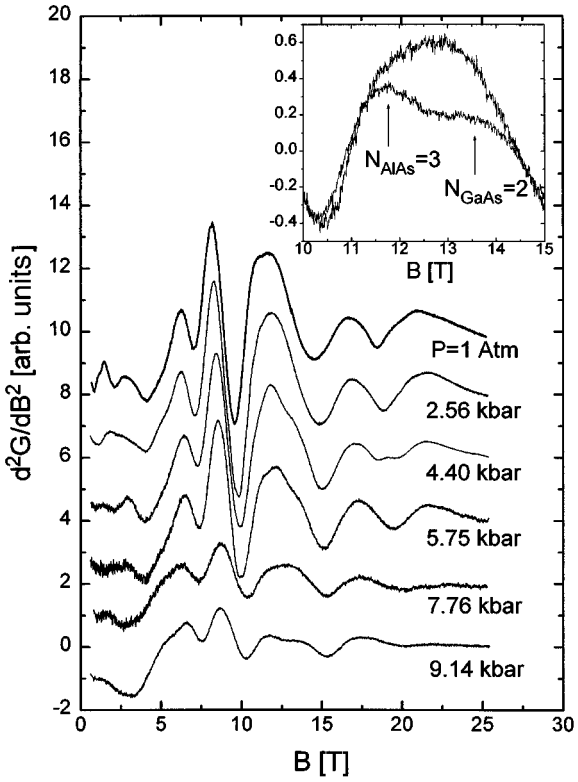

FIG. 9. Second derivative of the magnetoconductance of sample *A* under hydrostatic pressure up to 9.14 kbar at 150 K. In the inset, the splitting of the $N=3$ resonance of AlAs and the $N=2$ resonance of GaAs at pressures of 7.76 and 9.14 kbar is clearly observed.

Moreover, the maximum of the temperature dependence of these oscillations for voltages in the nonlinear regime shifts to higher temperature, probably due to the fact that, as explained above, this effect is no longer linearly dependent on the electron lifetime. To our knowledge, no reliable theory for superlattices is available.

D. Pressure dependence

In III-V semiconductors, the effect of hydrostatic pressure is to increase the direct gap and thus the Γ effective mass while decreasing the Γ-X energy separation. When this separation is small enough for the thermal activation to be efficient, electrons can be transferred from the Γ to the X band.[40] (Most experiments are done at temperatures where the thermally activated transfer to the X band is nonnegligible.) For GaAs/AlAs short-period superlattices, the effect of increasing hydrostatic pressure, observed through the Bloch transport, is to reduce the miniband width[41] with the increasing pressure. In addition, hydrostatic pressure modifies the relative energy separation between the Γ miniband, originating from the GaAs-Γ band edge, and the lowest Xz states, coming from the AlAs X-band edge. The result is a thermally activated transfer of electrons[41] from a high-mobility (low density of states) Γ region to a low-mobility (high density of states) Xz region.

The longitudinal magnetoconductance of sample *A* has been measured under hydrostatic pressure at 285 and 150 K. The change of the relative strengths of the two series under hydrostatic pressure allows us to demonstrate the superposition of the two series involving the LO phonon of GaAs and AlAs. In addition, we observe the disappearance of the magnetophonon resonances due to the Γ-X transfer of electrons. Figure 8 plots the second derivative of the magnetoconductance for a fixed voltage in the nonlinear regime, under hydrostatic pressure from ambient pressure to 10.65 kbar. Although the magnetoresistance decreases with increasing pressure, we observe that the relative amplitude of the resonances also decreases, which reflects the fact that the probability of transfer from Γ to Xz increases with increasing pressure. This means that electrons in the first Landau level preferentially undergo an interband scattering rather than optical phonon scattering, due to the high density of states of the final X band. Furthermore, the magnetophonon resonances are all shifted to higher magnetic field as the pressure increases. Both the in-plane effective mass and the optical phonon energy increase with hydrostatic pressure. The shift of the different resonance positions extracted from the second derivative is plotted in the inset of Fig. 8. We note that the two series have a different pressure dependence. From the $N=2$ positions of the AlAs series we have extracted a pressure coefficient for the peak shift of 0.3 $\mathrm{T\,kbar^{-1}}$, whereas the corresponding value for GaAs is between 0.21 and 0.22 $\mathrm{T\,kbar^{-1}}$. As the electrons involved in the scattering mechanisms have the same Γ in-plane effective mass, the difference must originate from the pressure dependence of the LO phonon energy. This difference is consistent with the pressure dependence of phonon modes in GaAs/AlAs superlattices.[42] From Brillouin and Raman scattering mea-

surements, it has been established that up to 150 kbar the LO phonon energy of GaAs increases linearly with the applied pressure as

$$\Delta\omega_{\mathrm{LO}} = r\frac{-\Delta a}{a_0}, \tag{16}$$

where $r = 120$ meV for GaAs and 159 meV for AlAs. $\Delta a/a_0$ is the relative variation of the bulk lattice parameter under hydrostatic pressure, which is nearly the same for both materials because their elastic constants are almost identical.

We have performed similar measurements at lower temperature (150 K) in order to reduce the effect of the thermally activated carrier transfer to the X states. Figure 9 plots the second derivative of the magnetoconductance for a fixed voltage in the nonlinear regime. As observed for the experiment at 285 K, the amplitude of the oscillations is reduced by the Γ-X transfer at high pressures and the resonances are shifted to higher magnetic field. The main feature is the broadening of the peak corresponding to the superposition of the $N=2$ resonance of the GaAs phonon and the $N=3$ resonance of the AlAs phonon at 7.76 kbar and the clear splitting observed at 9.14 kbar. Due to the different pressure dependences of the phonons, the different order of the resonances of the two series leads to a different shift in the magnetic field position with pressure, but above all the strength of the AlAs series increases, as the energy difference between the Γ miniband and the X states decreases due to the fact that a larger part of the Γ wave function penetrates into the AlAs barrier. As a consequence, the strength of the GaAs series decreases.

V. CONCLUSION

The magnetophonon effect has been investigated in the vertical magnetoconductance of short-period semiconductor superlattices. The presence of two superposed series of oscillations originating from the GaAs and the AlAs LO phonons has been demonstrated. The observed enhancement of the magnetophonon effect with the electric field is related to the high-velocity and low-density-of-states region in the middle of the Brillouin zone. The temperature dependence of the resonance confirms that our measurements are not in a hot-electron magnetophonon regime. The data are well explained by considering the competition between the phonon population and the electron lifetime. Hydrostatic pressure has been shown to be useful for separating the GaAs and AlAs series of oscillations by changing the relative strengths of each series as the energy of the Γ miniband approaches the X states.

ACKNOWLEDGMENTS

We are grateful to Dr. J.C. Vallier for assistance with the hybrid magnet, to H. Jones and his team for technical help with the pulsed magnet, and to Michel Rabary for technical support for the pressure measurements. We would like to thank also F. Mollot for the growth of some of the samples studied and also J.C. Esnault and S. Vuye for technical assistance in device processing. This work has been supported by Centre National de la Recherche Scientifique and by the Centre National d'Etudes des Télécommunications.

*Present address: Department ETRO, Vrije Universiteit Brussel, Pleinlaan 2, B-1050 Brussels, Belgium.

†Present address: High Magnetic Field Laboratory-CNRS, Boîte Postale 166, 38042 Grenoble, France.

‡Present address: Departmento de Física, Universidade Federal de São Carlos, C.P. 676, 13565-905 São Carlos, São Paulo, Brazil.

[1] V.L. Gurevitch and Yu.A. Firsov, Zh. Eksp. Teor. Fiz. **40**, 198 (1961) [Sov. Phys. JETP **13**, 137 (1961)].

[2] R.J. Nicholas, Prog. Quantum Electron. **10**, 1 (1985).

[3] D.C. Tsui, Th. Englert, A.Y. Cho, and C. Gossard, Phys. Rev. Lett. **44**, 341 (1980).

[4] J.C. Portal, J. Cisowski, R.J. Nicholas, M.A. Brummell, M. Razeghi, and M.A. Poisson, J. Phys. C **16**, L573 (1983).

[5] P. Warmenbol, F.M. Peeters, and J.T. Devreese, Phys. Rev. B **39**, 7821 (1989).

[6] S. Das Sarma, Phys. Rev. Lett. **52**, 859 (1984).

[7] R. Lassnig and W. Zawadskii, J. Phys. C **16**, 5435 (1983); Surf. Sci. **142**, 361 (1984).

[8] N. Mori, H. Murata, K. Taniguchi, and C. Hamaguchi, Phys. Rev. B **38**, 7622 (1988).

[9] N. Mori and T. Ando, Phys. Rev. B **40**, 6175 (1989).

[10] A. Suzuki, Phys. Rev. B **45**, 6731 (1992).

[11] H. Noguchi, H. Sakaki, T. Takamasu, and N. Miura, Phys. Rev. B **45**, 12 148 (1992).

[12] J.F. Palmier, *Resonant Tunneling in Semiconductors*, edited by L.L. Chang (Plenum, New York, 1991), p. 361.

[13] J. Genoe, K. Fobelets, C. Van Hoof, and G. Borghs, Phys. Rev. B **52**, 14 025 (1995); **53**, 13 194 (1996).

[14] E.D. Palik, G.S. Picus, S. Teitler, and R.F. Wallis, Phys. Rev. **122**, 475 (1961).

[15] C. Hermann and C. Weisbuch, Phys. Rev. B **15**, 823 (1977).

[16] G. Fasol, M. Tanaka, H. Sakaki, and Y. Horikoshi, Phys. Rev. B **38**, 6056 (1988).

[17] D.J. Mowbray, M. Cardona, and K. Ploog, Phys. Rev. B **43**, 1598 (1991).

[18] B. Jusserand and M. Cardona, in *Light Scattering in Solids V*, edited by M. Cardona and G. Guntherodt (Springer, Heidelberg, 1989).

[19] S. Adachi, J. Appl. Phys. **58**, R1 (1985).

[20] G.D. Mahan, *Many-Particle Physics* (Plenum, New York, 1990).

[21] N.M. Guseĩnov, Phys. Solid State **37**, 37 (1995).

[22] A. Sibille, J.F. Palmier, H. Wang, and F. Mollot, Phys. Rev. Lett. **64**, 52 (1990).

[23] H. Budd, Phys. Rev. **127**, 4 (1962).

[24] V.M. Polyanovskii, Fiz. Tekh. Poluprovodn. **14**, 1215 (1980) [Sov. Phys. Semicond. **14**, 718 (1980)].

[25] J.F. Palmier, A. Sibille, G. Etemadi, A. Celeste, and J.C. Portal, Semicond. Sci. Technol. **7**, B283 (1992).

[26] A. Sibille, J.F. Palmier, A. Celeste, J.C. Portal, and F. Mollot, Europhys. Lett. **13**, 279 (1990).

[27] H.J. Hutchinson, A.W. Higgs, D.C. Herbert, and G.W. Smith, J. Appl. Phys. **75**, 320 (1994).

[28] J.R. Barker, J. Phys. C **5**, 1657 (1972).

[29] J.S. Blakemore and J.A. Kennewell, J. Phys. C **8**, 647 (1975).

[30] L. Canali, M. Lazzarino, L. Sorba, and F. Beltram, Phys. Rev. Lett. **76**, 3618 (1996).

[31] H.T. Grahn, K. von Klitzing, K. Ploog, and G.H. Dolher, Phys. Rev. B **43**, 12 094 (1991).
[32] N. Kotera, K.F. Komatsabara, and E. Yamada, in *Proceedings of the International Conference on Physics of Semiconductors, Kyoto 1966*, edited by K. Kinosita (The Physical Society of Japan, Tokyo, 1966), p. 411.
[33] M.M. Akselrod and I.M. Tsidilkovskii, Pis'ma Zh. Eksp. Teor. Fiz. **9**, 622 (1969) [JETP Lett. **9**, 381 (1969)].
[34] P. Warmenbol, F.M. Peeters, X. Wu, and J.T. Devreese, Phys. Rev. B **40**, 6258 (1989).
[35] R.A. Suris and B.S. Shchamkhalova, Fiz. Tekh. Poluprovodn. **18**, 1178 (1984) [Sov. Phys. Semicond. **18**, 738 (1984)].
[36] C. Minot, H. Le Person, J.F. Palmier, and F. Mollot, Phys. Rev. B **47**, 10 024 (1993).
[37] L. Eaves, P.S.S. Guimaraes, J.C. Portal, T.P. Pearsall, and G. Hill, Phys. Rev. Lett. **53**, 608 (1984).
[38] P. Vasilopoulos, M. Charbonneau, and C.M. Van Vliet, Phys. Rev. B **35**, 1334 (1987).
[39] R.A. Stradling and R.A. Wood, J. Phys. C **3**, L94 (1970).
[40] G.D. Pitt and J. Lees, in *Colloques Internationaux du Centre National de la Recherche Scientifique, Grenoble, 1970*, edited by G. Roland (CNRS, Grenoble, 1970), p. 225.
[41] P. Gassot, L. Dmowski, M. Eremets, F. Aristone, B. Goutiers, J.L. Gauffier, D.K. Maude, J.F. Palmier, J.C. Portal, J.C. Harmand, and F. Mollot, Solid State Electron. **40**, 185 (1996).
[42] P. Seguy, J.C. Maan, G. Martinez, and K. Ploog, Phys. Rev. B **40**, 1598 (1989).